PCCP

PAPER

View Article Online
View Journal | View Issue



Cite this: *Phys. Chem. Chem. Phys.*, 2015, **17**, 29335

# Oriented polyvinylidene fluoride–trifluoroethylene (P(VDF–TrFE)) films by Langmuir–Blodgett deposition: a synchrotron X-ray diffraction study

W. R. Lindemann,[abc] R. L. Philiph,[ad] D. W. W. Chan,[e] C. T. Ayers,[e] E. M. Perez,[a] S. P. Beckman,[af] J. Strzalka,[g] S. Chaudhary[e] and D. Vaknin*[bh]

Received 23rd July 2015,
Accepted 6th October 2015

DOI: 10.1039/c5cp04307g

www.rsc.org/pccp

Langmuir–Blodgett films of polyvinylidene fluoride trifluoroethylene – P(VDF–TrFE)-copolymers possess substantially improved electrocaloric and pyroelectric properties, when compared with conventionally spin-cast films. In order to rationalize this, we prepared single-layered films of P(VDF–TrFE) (70 : 30) using both deposition techniques. Grazing incidence wide-angle X-ray scattering (GIWAXS), reveals that Langmuir–Blodgett deposited films have a higher concentration of the ferroelectric β-phase crystals, and that these films are highly oriented with respect to the substrate. Based on these observations, we suggest alternative means of deposition, which may substantially enhance the electrocaloric effect in P(VDF–TrFE) films. This development has significant implications for the potential use of P(VDF–TrFE) in solid-state refrigeration.

## Introduction

Polyvinylidene fluoride (PVDF) and its copolymers have received increasing interest in recent years, due to their tremendous potential for use in solid-state, electrocaloric refrigeration. Unlike traditional thermoelectric cooling systems, *i.e.*, Peltier devices, which rely on permanent voltage gradients, pyroelectric materials such as PVDF experience internal temperature changes due to cyclic variations of applied voltage.[1–6] Pyroelectrics, traditionally only used in sensors, recaptured the interest of the scientific community in 2006, when the first 'giant' electrocaloric effect was reported in ceramic thin films.[7] Similar interest was drawn from the polymer-science community when Neese *et al.* observed a comparable electrocaloric temperature change of 12 °C in films of poly(vinylidene fluoride–trifluoroethylene) (abbreviated: P(VDF–TrFE)).[8]

Since the work of Neese *et al.*, numerous attempts have been made to enhance the electrocaloric temperature change of P(VDF–TrFE), resulting in temperature changes as large as 35 °C.[5,6,9,10] However, most of these efforts require modification of existing crystallographic domains using intense irradiation or copolymerization. In one notable study, Liu *et al.* improved the morphology of P(VDF–TrFE) (70 : 30) by employing Langmuir–Blodgett (LB) deposition to produce highly uniform multilayered films.[11] This deposition method resulted in electrocaloric temperature changes of 21 °C, whereas conventionally spin-cast films of the same polymer exhibit temperature changes closer to 12 °C.[5,11]

In LB-deposition a uniform layer of P(VDF–TrFE) polymer is spread on the surface of water. A substrate is lowered and raised through this layer to deposit the polymer layer by layer. This technique can be used to produce films that are homogeneous with an arbitrary thickness based on the number of layers deposited. LB-deposition is well-known to affect the ferroelectric properties of PVDF copolymers. For instance, Ducharme *et al.* have shown that LB-deposition decreases the zero-field phase transition temperature of P(VDF–TrFE) (70 : 30) by more than 20 °C.[12]

The crystal structure and electronic properties of P(VDF–TrFE) polymers are well-characterized. Gregorio Jr. and Botta published a phase-diagram for this copolymer which indicates that when deposited at room-temperature, P(VDF–TrFE) can exist in two primary, phases: α and β.[13] The β phase is ferroelectric, resulting from an all-*trans* (TTTT) configuration of polymer chains. The α phase is paraelectric, resulting from an antiparallel (TGTḠ) configuration of polymer chains.[14] An additional paraelectric γ phase is observed sometimes; however, this is rare at room temperature.[13] X-ray diffraction (XRD) is the most reliable

[a] *Department of Materials Engineering, Iowa State University, Ames, IA 50011, USA*
[b] *Ames National Laboratory, Ames, IA 50011, USA. E-mail: vaknin@ameslab.gov*
[c] *Department Materials Science & Engineering, Massachusetts Institute of Technology, Cambridge, MA 02139, USA*
[d] *Department Bioengineering, University of Washington, Seattle, WA 98105, USA*
[e] *Department of Electrical & Computer Engineering, Iowa State University, Ames, IA 50011, USA*
[f] *School of Mechanical and Materials Engineering, Washington State University, Pullman, WA 99164, USA*
[g] *X-Ray Science Division, Argonne National Laboratory, Argonne, Illinois, USA*
[h] *Department of Physics and Astronomy, Iowa State University, Ames, IA 50011, USA*

method to distinguish between these phases (since peak positions are well-established for the α and β phases of P(VDF–TrFE)), although infrared spectroscopy may also be used to identify them.[15]

Liu *et al.* attribute the electrocaloric enhancement of LB films to improved polymer crystallinity, based on their XRD measurements.[11] Other authors have also characterized LB-films using XRD techniques.[16] However, there have been no reports characterizing the crystallographic orientation within the films, which likely has a major role in determining the electrocaloric behaviour. In this manuscript grazing incidence wide-angle X-ray scattering (GIWAXS) using synchrotron radiation is used to determine the crystalline order of single-layer films of P(VDF–TrFE) (70 : 30). LB-deposited and spin-cast films are compared to rationalize the enhanced electrocaloric effect observed in LB-deposited films.

## Experimental section

### Materials

P(VDF–TrFE) (70 : 30) was purchased in powder form from Piezotech, and was used without further purification. Solutions of this polymer were prepared by dissolving the powder in dimethyl formamide (DMF) for LB-deposition and in dimethyl sulfoxide (DMSO) for spin-coating. Lattice parameters for this composition are $a$ = 9.86 Å and $c$ = 2.30 Å for the hexagonal α-phase and $a$ = 9.05 Å, $b$ = 5.12 Å and $c$ = 2.55 Å for the quasi-hexagonal β-phase.[17] These chemicals were purchased from Fisher Scientific and BDH respectively, both with >99.9% purity. Both were used without further modification. The difference in solvents during deposition was not considered significant, since the solvent evaporates completely prior to the start of Langmuir–Blodgett deposition. Samples were deposited on silicon wafers, which were sectioned using a diamond-scribe. Ultrapure water (Milli-pore, Milli-Q, 18.2 MΩ cm) was used during the Langmuir–Blodgett deposition process to avoid contamination.

### Langmuir–Blodgett (LB) deposition

Langmuir–Blodgett deposition was performed using a Nima Langmuir–Blodgett Trough Type 611 and a Nima Dipper Mechanism Type D1L. A P(VDF–TrFE) solution with a concentration of 0.48 g $L^{-1}$ was prepared by dissolving the polymer in DMF. Ultrapure water was poured into the Nima trough and 270 μL of the P(VDF–TrFE) solution was spread at the interface using a pipette.

The surface-pressure of the solution was continuously monitored and, after a 10 minute wait-time, the surface was compressed to a surface pressure of $\Pi$ = 5.3 mN $m^{-1}$. The surface pressure was measured using a Wilhelmy plate and was calibrated using arachidic acid solution, which experiences several well-defined phase transitions during compression isotherms.[18] The target pressure, once reached, was maintained while the silicon substrate was raised through the polymer film, slowly depositing a single layer on the substrate surface. Finally, the substrate was removed, the position of the film was marked, and the substrate was allowed to dry. The film-thickness was approximated as 1–2 nm thick, which agrees with Ducharme's observed 1.78 nm layer-thickness for LB-deposited P(VDF–TrFE) (70 : 30) films.[19] Deposition of multiple layers was attempted. However, optical microscopy revealed that this caused aggregation of the polymer, meaning that true multilayers were not produced. Therefore, these films were disregarded. Based on Ducharme's observation that LB-layers of this co-polymer are highly uniform, we argue that the crystalline properties of a single layer are comparable to the properties of multilayered films.[19]

### Spin-coating

Spin-coated films were produced using a solution of 5 wt% P(VDF–TrFE) in DMSO. This solution was spread on a silicon substrate and the substrate was rotated at 4250 rpm. The film's thickness was determined using a Filmetrics model F20 spectrophotometer. This instrument is capable of measuring films ranging from 15 to 70 000 nm in thickness, and can use a wavelength range of 380–1500 nm. Uniformity of the film was verified using optical microscopy.

### Grazing incidence wide-angle X-ray scattering (GIWAXS)

GIWAXS measurements of the films described above were performed at Beamline 8-ID-E of the Advanced Photon Source (APS) at Argonne National Laboratory.[20] The photon energy was 7.35 keV. Scattering patterns were measured using a Pilatus 1 M pixel array detector (1043 × 981 pixels; Dectris) and the data were analyzed using the GIXSGUI software package[21] for Matlab (Mathworks) (available for download at https://www1.aps.anl.gov/Sectors/Sector-8/8-ID/Operations-and-Schedules/Useful-Links/Sector-8-GIXSGUI). The pixel size is 172 μm by 172 μm and the sample-to-detector distance is 204.5 mm. Incident angles of 0.14°, 0.17° and 0.20° were used, since these provided measurements below, near and above the critical angle of the organic layer. The length of both samples exceeded 3.0 cm. The X-ray beam-size was defined by slits. The vertical beam width was 20 μm, the horizontal beam width was 200 μm and the maximum beam footprint was 8.18 mm. A vacuum sample chamber with large Kapton exit window and internal beamstop maintained the sample under vacuum so as to minimize radiation damage and parasitic scattering.

At each incident angle, we recorded scattering patterns with the detector at two distinct vertical positions. These pairs of images were corrected for detector non-uniformity and bad pixels, and then combined to fill in rows of inactive pixels at the junctions between modules comprising the detector active area. Further corrections for pixel energy sensitivity, geometry and polarization were also applied before mapping the data from pixel-space into reciprocal space (**q**-space). The absence of artifacts in the combined two-dimensional scattering patterns demonstrates that the samples did not experience radiation damage during exposure to the beam.

The two-dimensional data were reshaped for display as scattered intensity as a function of the photon wave-vector transfer in the plane of the sample $q_r = \sqrt{q_x^2 + q_y^2}$ and out of the plane of the sample ($q_z$). This representation makes it

obvious that in a GIWAXS measurement scattering information in a wedge along the $q_z$-axis is not observed.[22,23] Another advantage of this representation is that the scattered intensity along the polar angle $\chi$ is a partial pole-figure for the sample. The dark region in the upper left of GIWAXS images is caused by the size of the Kapton exit window. The dark thin ribbon near $q_r = -1$ Å$^{-1}$ is due to columns of inactive pixels left uncompensated for after vertical displacement of the detector.

Images were recorded from 2–3 distinct regions of each sample, verifying the homogeneity of the thin film samples.

## Results and discussion

### Langmuir–Blodgett deposition

Prior to LB-deposition, a surface-pressure isotherm test was measured to ensure that the P(VDF–TrFE) layer behaves normally at the air–water interface. Although typically surface pressure ($\Pi$) is compared to molecular area, in this case the film consisted of a copolymer and the meaning of 'molecular area' is not well-defined. Instead a simple plot of $\Pi$ *versus* trough area ($A$) is displayed in Fig. 1. Qualitatively, this isotherm agrees well with that of Liu *et al.*[11] This measurement was reproduced several times. An estimation of molecular area can be produced by assuming that a P(VDF–TrFE) 'molecule' has the weighted-average molecular weight of the VDF and TrFE monomers. This analysis suggests that our polymer has a lower molecular area than the polymer used by Liu *et al.*, presumably indicating that some material adhered to the trough-wall. However, the stability and reproducibility of the isotherm in Fig. 1 attest to the presence of a uniform polymer layer at the air–water interface. A first-order approximation of film thickness can be computed by assuming that the P(VDF–TrFE) film has uniform thickness ($t$) given by eqn (1)

$$t = \frac{\Delta A}{A_0} \times \frac{C \times V}{\delta} \times \frac{1}{A_s} \quad (1)$$

where $\Delta A$ is the change in area during deposition, $A_0$ is the initial trough area during deposition, $C$ is the concentration of the P(VDF–TrFE) solution (g L$^{-1}$), $V$ is the volume of solution, $\delta$ is the density of the polymer, and $A_s$ is the area of the substrate. Using this approximation the film is determined to be 1–2 nm thick, in agreement with the literature.[11,24]

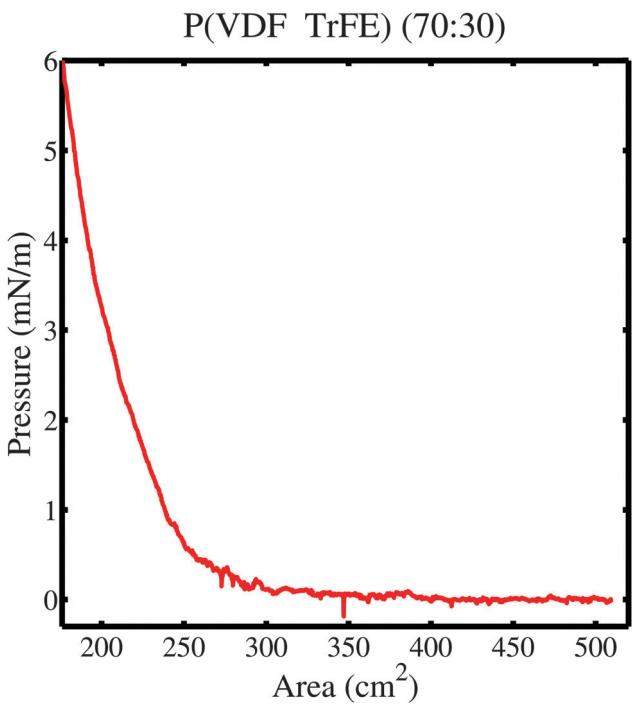


Fig. 1 A surface pressure–area isotherm for P(VDF–TrFE) at the surface of water prior to Langmuir–Blodgett deposition.

### Spin-coating

Two polymer films were cast using the parameters described in the experimental section. These films were studied using an optical microscope and determined to be uniform. Using UV/VIS spectroscopy and averaging over three sites, their thicknesses were determined to be 61.16 ± 0.16 nm and 59.46 ± 0.74 nm. This indicates that spin-coated films were uniform. A few pinholes were observed in both films; however, these were considered unlikely to affect X-ray measurements.

### Grazing incidence wide-angle X-ray scattering (GIWAXS)

2-Dimensional diffraction-patterns from both LB-deposited and spin-coated P(VDF–TrFE) films are shown in Fig. 2. Fig. 2(a) shows a 2D diffraction image from the LB-deposited film; Fig. 2(b) shows a 2D diffraction image from the spin-coated film. The pseudo-hexagonal diffraction pattern from LB-deposited films, which corresponds to either the (110) or the (200) plane of the β-phase crystals, indicates that one of these planes is oriented perpendicular to the silicon substrate, *i.e.*, the polymer chains are oriented parallel to the substrate. Because these planes have similar lattice-spacings, it is impossible to distinguish between them using these results. However, these peaks are in good agreement with diffraction peaks observed in previous studies.[14,25,26] No additional diffraction peaks were observed for either the α- or the γ-phase, suggesting that only β-phase P(VDF–TrFE) is present in the LB films.

In contrast, the diffraction pattern from the spin-coated films demonstrates a nearly isotropic texture, as evidenced by the circular diffraction pattern. In some cases, a small degree of anisotropy was detected; however, no spin-cast film came close to exhibiting the anisotropic scatter pattern demonstrated in Fig. 2(a). Another key difference between the two diffraction patterns is the presence of a secondary peak in the spin-coated films. This peak likely corresponds to the (110) plane of the α-phase of P(VDF–TrFE). Another peak, belonging to the (020) and the (100) planes of the α-phase was expected; however, because the (110) peak is more intense and very broad, these peaks may have been overwhelmed by signal from the α (110) planes. This observation agrees with the findings of Koga *et al.*, who observed a very similar diffraction pattern while studying P(VDF–TrFE) (82 : 18) films.[14]

To make this comparison more obvious, a plot of intensity *vs.* $q$ (where $q = \|\mathbf{q}\|$) was produced by integrating the left half of

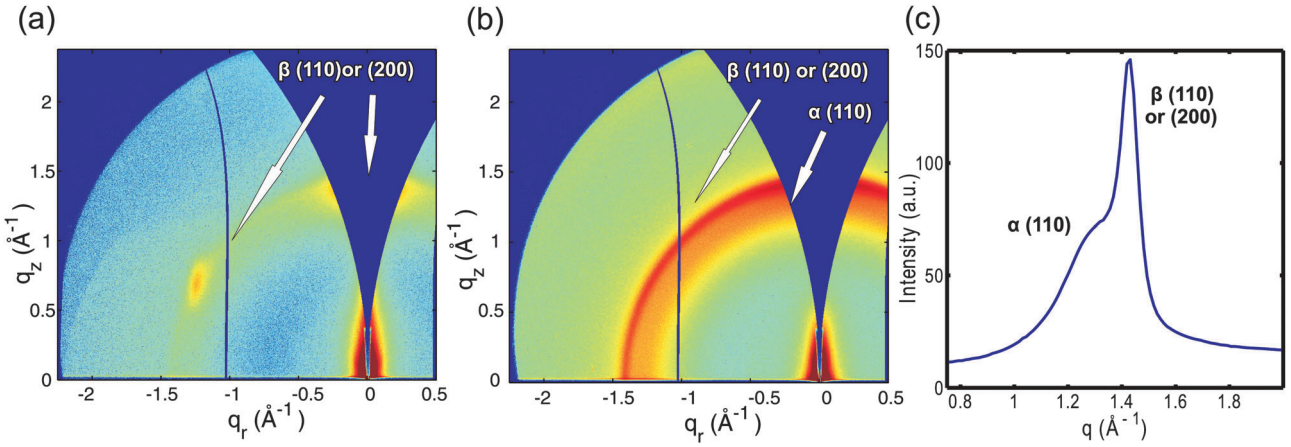


Fig. 2 (a and b) GIWAXS diffraction image from (a) an LB-deposited P(VDF–TrFE) (70 : 30) film; (b) a spin-coated film. Only highly-oriented β-phase material is observed in (a), whereas randomly oriented β-phase and α-phase is observed in (b). This difference indicates substantial changes in the films' structural properties. (c) Integrated intensity of (b) as a function of $q$.

Fig. 2(b). This profile can be compared to normal $2\theta$ diffraction profiles using the equation

$$\|\mathbf{q}\| = \frac{4\pi}{\lambda}\sin(\theta) \qquad (2)$$

where $2\theta$ is the scattering angle and $\lambda$ is the diffraction wavelength. This is shown in Fig. 2(c). A similar figure is not given for LB-deposited film because this diffraction profile is so anisotropic.

These diffraction results suggest two mechanisms for the superior pyroelectric performance of LB-deposited films compared to the spin-cast ones. First, the LB-deposited films have greater phase purity of the ferroelectric β-phase. The α-phase, which is clearly observed in spin-cast films, is paraelectric, and its presence reduces the polarizability of the polymer film. Second, the crystals in the LB-deposited P(VDF–TrFE) films are strongly textured. This anisotropy tends to enhance the polarizability of LB-deposited films in the out-of-plane direction.

Langmuir–Blodgett deposition is an inefficient method of producing large scale P(VDF–TrFE) thin films; however, reproducing the effects observed in LB films should be possible using more broadly-available techniques. For instance, Koga *et al.* demonstrated that repeated polarization of P(VDF–TrFE) films during annealing can enhance the phase-fraction of β in spin-cast films, producing films of entirely β-phase P(VDF–TrFE).[14] By rapid annealing of PVDF films on gold substrates, Kang *et al.* formed β-phase films with a crystalline texture similar to the texture displayed in Fig. 2(a).[26]

## Conclusions

In summary, we produced single-layer P(VDF–TrFE) (70 : 30) thin films using Langmuir–Blodgett deposition and spin-coating. In order to rationalize the exceptional performance of LB-deposited films for electrocaloric and pyroelectric applications, we studied these films using grazing incidence wide-angle X-ray scattering (GIWAXS). We report the surface-pressure isotherm for the co-polymer, along with the GIWAXS analysis of both films. The obvious crystallographic texturing of LB-deposited films, as well as these films' increased fraction of the polymer's ferroelectric β-phase, led us to conclude that these two mechanisms may explain the enhanced electrocaloric temperature change observed by Liu *et al.* While this finding is promising, we point out that further experiments are needed to prove that this structure is preserved in multi-layered films. Finally, we note that uniform films with both of these properties may be produced using alternative deposition techniques described by Koga and Kang, which are more scalable, convenient methods of processing P(VDF–TrFE).[14,26] We argue that these techniques could lead to substantial improvements in the electrocaloric effect of polymers for use in solid-state refrigeration.

## Acknowledgements

Ames Laboratory is funded by the Office of Basic Energy Sciences, U.S. Department of Energy under Contract No. DE-AC02-07CH11358. Scott P. Beckman is grateful to the National Science Foundation for support through grant DMR-1105641. We gratefully acknowledge Peter Onstad's support for this work. This research used resources of the Advanced Photon Source, a U.S. Department of Energy (DOE) Office of Science User Facility operated for the DOE Office of Science by Argonne National Laboratory under Contract No. DE-AC02-06CH11357.

## References

1 R. B. Olsen, D. a. Bruno, J. M. Briscoe and E. W. Jacobs, *J. Appl. Phys.*, 1985, **57**, 5036–5042.
2 R. C. Moreno, B. a. James, A. Navid and L. Pilon, *Int. J. Heat Mass Transfer*, 2012, **55**, 4301–4311.
3 H. Nguyen, A. Navid and L. Pilon, *Appl. Therm. Eng.*, 2010, **30**, 2127–2137.
4 F. Y. Lee, A. Navid and L. Pilon, *Appl. Therm. Eng.*, 2012, **37**, 30–37.

 

5 S. G. Lu, B. Rožič, Q. M. Zhang, Z. Kutnjak, X. Li, E. Furman, L. J. Gorny, M. Lin, B. Malič, M. Kosec, R. Blinc and R. Pirc, *Appl. Phys. Lett.*, 2010, **97**, 6–9.
6 X. Li, X. S. Qian, H. Gu, X. Chen, S. G. Lu, M. Lin, F. Bateman and Q. M. Zhang, *Appl. Phys. Lett.*, 2012, **101**, 2010–2014.
7 A. S. Mischenko, Q. Zhang, J. F. Scott, R. W. Whatmore and N. D. Mathur, *Science*, 2006, **311**, 1270–1271.
8 B. Neese, B. Chu, S.-G. Lu, Y. Wang, E. Furman and Q. M. Zhang, *Science*, 2008, **321**, 821–823.
9 S. G. Lu, B. Rozic, Q. M. Zhang, Z. Kutnjak and R. Pirc, *Appl. Phys. A: Mater. Sci. Process.*, 2012, **107**, 559–566.
10 S. Lu and Q. Zhang, *Adv. Mater.*, 2009, **21**, 1983–1987.
11 P. F. Liu, J. L. Wang, X. J. Meng, J. Yang, B. Dkhil and J. H. Chu, *New J. Phys.*, 2010, **12**, 023035.
12 S. Ducharme, A. Bune, L. Blinov, V. Fridkin, S. Palto, A. Sorokin and S. Yudin, *Phys. Rev. B*, 1998, **57**, 25–28.
13 R. Gregorio Jr. and M. M. Botta, *J. Polym. Sci.*, 1998, **36**, 403–414.
14 K. Koga, N. Nakano, T. Hattori and H. Ohigashi, *J. Appl. Phys.*, 1990, **67**, 965–974.
15 M. Benz and W. B. Euler, *J. Appl. Polym. Sci.*, 2003, **89**, 1093–1100.
16 J. Kim, H. You, S. Ducharme and S. Adenwalla, *J. Phys.: Condens. Matter*, 2007, **19**, 086206.
17 E. Bellet-Amalric and J. F. Legrand, *Eur. Phys. J. B*, 1998, **3**, 225–236.
18 Y. S. Kang, D. K. Lee, C. S. Lee and P. Stroeve, *J. Phys. Chem. B*, 2002, **106**, 9341–9346.
19 S. Ducharme, T. J. Reece, C. M. Othon and R. K. Rannow, *IEEE Trans. Device Mater. Reliab.*, 2005, **5**, 720–735.
20 Z. Jiang, X. Li, J. Strzalka, M. Sprung, T. Sun, A. R. Sandy, S. Narayanan, D. R. Lee and J. Wang, *J. Synchrotron Radiat.*, 2012, **19**, 627–636.
21 Z. Jiang, *J. Appl. Crystallogr.*, 2015, **48**, 917–926.
22 J. L. Baker, L. H. Jimison, S. Mannsfeld, S. Volkman, S. Yin, V. Subramanian, A. Salleo, A. P. Alivisatos and M. F. Toney, *Langmuir*, 2010, **26**, 9146–9151.
23 J. Rivnay, S. C. B. Mannsfeld, C. E. Miller, A. Salleo and M. F. Toney, *Chem. Rev.*, 2012, **112**, 5488–5519.
24 S. Palto, L. Blinov, A. Bune, E. Dubovik, V. Fridkin, N. Petukhova, K. Verkhovskaya and S. Yudin, *Ferroelectr., Lett. Sect.*, 1995, **19**, 65–68.
25 V. Gelfandbein and M. M. Perlman, *J. Mater. Sci.*, 1983, **18**, 3183–3189.
26 S. J. Kang, Y. J. Park, J. Sung, P. S. Jo, C. Park, K. J. Kim and B. O. Cho, *Appl. Phys. Lett.*, 2008, **92**, 012921.